

Concentration Dependence of Static and Dynamic Properties for Polymeric Stars in a Good Solvent

Mireille Adam,^{*,1a} Lewis J. Fetters, William W. Graessley,^{*,1b} and Thomas A. Witten^{1c}

Corporate Research Laboratories, Exxon Research and Engineering Company, Annandale, New Jersey 08801

Received July 26, 1990; Revised Manuscript Received November 14, 1990

ABSTRACT: Equilibrium and dynamical properties were obtained by light scattering methods for solutions of multiarm polyisoprene star polymers in a good solvent, cyclohexane, over a wide concentration range. Results for 8-arm and 18-arm stars were compared with the behavior of linear polymers in the dilute and semidilute regimes and were analyzed in terms of recent theories based on the Daoud-Cotton model. In dilute solutions the temporal fluctuations on distance scales smaller than the overall dimensions were found to be markedly slower for stars than for linear chains of the same size. Evidence for star-star repulsion and liquidlike ordering near the overlap concentration was also obtained. Such differences between linear polymers and stars vanish in the semidilute region, however, with the osmotic pressure derivative and mutual diffusion coefficient becoming power law functions of the polymer concentration alone. The scaling law prefactors depend on the arm number but less strongly than predicted by theory.

Introduction

Multiarm star molecules have been used for many years to study the influence of long branches on a variety of polymer properties. However, molecules with this structure—consisting of f linear chains with molecular weight M_a , linked at one end to a common junction to give a total molecular weight $M = fM_a$ —also provide a convenient means for exploring the effects of internal segment density on polymer solution behavior. Daoud and Cotton² have proposed a model to account for those effects in good solvents and under Θ conditions. They developed expressions for static properties such as radius of gyration, R_G , and osmotic pressure, π , in both dilute solutions, $c \ll c^*$, and semidilute solutions, $c \gg c^*$, where c is the polymer concentration and $c^* \propto M/R_G^3$ is the concentration at overlap. Other authors have extended their model, considering dynamical properties in the dilute regime^{3,4} as well as some special features of star polymer interactions near the overlap concentration.⁵ Some related experimental studies have been published.⁶⁻¹² The present paper reports an experimental investigation of concentration dependence in good solvents. Static and dynamical properties for linear and multiarm ($f = 8$ and 18) polyisoprenes in cyclohexane were obtained by light scattering methods. Results in dilute, semidilute, and overlap regimes are described. Differences in behavior between linear and star polymers, related to the differences in internal segment density, are discussed in relation to the Daoud-Cotton model.

Theoretical Background

According to the Daoud-Cotton picture, a multiarm star in dilute solution consists of a dense central core and a more tenuous outer region. The core radius b depends only on the number of arms ($b \propto f^{1/2}$) and is small compared with the overall dimensions, $b \ll R_G$, for sufficiently long arms. They model the outer region as a semidilute solution of chain segments with a correlation length $\xi(r)$ that increases with distance from the core, $\xi(r) \propto rf^{-1/2}$. In good solvents, $\xi(r)$ is the screening length for excluded-volume interactions, so each correlation volume $\xi^3(r)$ contains essentially a single self-avoiding segment. (According to ref 4, $\xi(r)$ also provides the screening length for hydrodynamic interactions.) This picture leads to an expression

for the overall dimensions of the star in dilute solution

$$R_G \sim (R_G)_a f^{(1-\nu)/2} \quad (1)$$

or

$$R_G \sim (R_G)_L f^{(1-3\nu)/2} \quad (2)$$

where $(R_G)_a$ and $(R_G)_L$ are the respective radii for an unattached arm and for a linear polymer with the same total molecular weight as the star. The exponent ν relates size and molecular weight for linear chains, $R_g \propto M^\nu$, with $\nu = 0.588$ for self-avoiding chains.¹³ For a constant total molecular weight, the overlap concentration increases with arm number. From eq 2 and with $c^* \propto M/R_G^3$

$$c^* \sim (c^*)_L f^{3(3\nu-1)/2} \quad (3)$$

which gives $c^* \sim (c^*)_L f^{1.146}$ for $\nu = 0.588$.

For semidilute solutions ($c^* \ll c \ll \rho$, where ρ is the density of undiluted polymer) the model assumes the polymer concentration is uniform (except in the dense but relatively small core regions), with a correlation length $\xi \propto c^{\nu/(1-3\nu)}$ and osmotic pressure

$$\pi \sim kT/\xi^3 \quad (4)$$

that are independent of chain architecture. Thus, linear polymers and star polymers with the same total molecular weight have the same osmotic pressure in dilute solutions, $\pi = cRT/M$, and also in semidilute solutions, $\pi \propto c^{3\nu/(3\nu-1)}$. However, c^* increases with f (eq 3), so as a result the osmotic pressure for stars must begin to rise rapidly with concentration near c^* in order finally to reach the architecture-independent power law in the semidilute regime. Noting the enhancement of $\partial\pi/\partial c$ near c^* , the authors of ref 5 pointed out that this would imply a thermodynamic repulsion between polymeric stars, a result of their high segment density, and suggested that a liquidlike ordering of the star molecules would occur near c^* if f were large enough.

Many of these predictions can be tested with light scattering data. At low concentrations ($c \ll \rho$) the polymeric static structure factor $S(q, c)$ can be determined from measurements of scattering intensity as a function

of scattering angle and concentration. Thus

$$S(q,c) = \Delta R(q,c)/Kc \quad (5)$$

where $\Delta R(q,c)$ is the excess Rayleigh ratio above that of pure solvent, $q = (4\pi/\lambda) \sin(\theta/2)$ is the magnitude of the scattering vector, θ is the scattering angle, λ is the wavelength of light in the medium, and K is a contrast factor, which can be obtained from independent measurements. For random solutions $S(q,c)$ is a monotonically decreasing function of q , but if the multiarm stars are locally ordered near c^* , as suggested in ref 5, then the static structure factor should increase with q initially and then pass through a maximum near $q = R_G^{-1}$.

For small scattering angles ($q\xi < 1$, or $qR_G < 1$ dilute solution)

$$S(q,c)^{-1} = \frac{1}{RT} \frac{\partial \pi}{\partial c} (1 + \alpha(c) q^2 + \dots) \quad (6)$$

where R is the universal gas constant, T is the temperature, and $\alpha(c)$ may be either positive or negative depending on the system. In the dilute range ($c \ll c^*$)

$$\alpha(0) = R_G^2/3 \quad (7)$$

and

$$\frac{\partial \pi}{\partial c} = \frac{RT}{M} (1 + 2A_2Mc + \dots) \quad (8)$$

where A_2 is the second virial coefficient. Thus, information on the concentration dependence of osmotic pressure can be obtained over the range of interest by extrapolations to zero scattering angle (eq 6). The values of M , R_G , and MA_2 can of course be obtained from scattering data in the dilute range (eqs 7 and 8) and can be used to locate the overlap concentration

$$c^* = M/N_a R_G^3 \quad (9)$$

or

$$c^* = (A_2M)^{-1} \quad (10)$$

where N_a is Avogadro's number.

In the semidilute range ($c \gg c^*$)

$$\alpha(c) = \xi^2 \quad (11)$$

and

$$\partial \pi / \partial c \propto RTc^{1/(3\nu-1)} \quad (12)$$

For linear polymers in the semidilute regime it has been established^{14,15} that the osmotic pressure is dependent only on concentration and obeys a scaling law

$$\frac{\pi}{\pi_0} \sim \frac{\partial \pi / \partial c}{(\partial \pi / \partial c)_0} \sim \left(\frac{c}{c^*} \right)^{1/(3\nu-1)} \quad (13)$$

For stars, the reduced osmotic pressure derivative is predicted to depend on the number of arms as $f^{3/2}$.⁵

Information about the dynamic structure factor can be obtained from the first cumulant of the intensity correlation function:¹⁶

$$D(q,c) = \Gamma(q,c)/2q^2 \quad (14)$$

For small scattering angles ($q\xi < 1$, or $qR_G < 1$ in dilute solution)

$$D(q,c) = D(c) (1 + \beta(c) q^2 + \dots) \quad (15)$$

where $D(c)$ is the mutual diffusion coefficient. In the dilute

range ($c \ll c^*$)

$$D(c) = D_0(1 + k_Dc + \dots) \quad (16)$$

where D_0 is the center of gravity diffusion coefficient and

$$\beta(0) = \kappa R_G^2 \quad (17)$$

where k_D depends on both the thermodynamic and frictional interactions of the scatterers ($k_D = 2A_2M - k_s$, where k_s governs the concentration dependence of the polymeric friction coefficient¹⁷). The dimensionless coefficient κ characterizes the internal dynamics, being of order 10^{-1} for flexible linear polymers and zero for rigid scatterers.

For large scattering angles ($q\xi > 1$ or $qR_G > 1$), it has been shown^{18,19} for linear polymers that eq 15 is no longer valid, and

$$D(q,c) \sim \frac{kT}{6\pi\eta} q \quad (18)$$

In dilute solutions, however, the association of $\xi(r)$ with internal hydrodynamic screening in stars⁴ suggests that κ would be much smaller for multiarm stars ($f \gg 1$) than for the corresponding linear polymers.

The Daoud-Cotton model implies that $D(c)$ is the same for linear polymers and multiarm stars in the semidilute regime.

$$D(c) = kT/6\pi\eta\xi(c) \propto c^{\nu/(3\nu-1)} \quad (19)$$

The mutual diffusion coefficient of linear polymers obeys a scaling law

$$D(c)/D_0 = (c/c^*)^{\nu/(3\nu-1)} \quad (19a)$$

One can easily show from eq 3 that the reduced mutual diffusion coefficient of star polymers depends on the number of arms as $f^{1/2}$.

The mobility per unit mass of polymer in the scattering volume q^{-3} is defined as (ref 18, p 210)

$$\mu(q,c) = S(q,c) D(q,c)/RT \quad (20)$$

where, from eqs 6 and 16

$$\mu(0,0) = D_0/MRT \equiv \mu_0 \quad (21)$$

For linear polymers in dilute solution

$$\mu(q,0) \propto q^{1-1/\nu} \quad (22)$$

when $qR_G \gg 1$. The same proportionality is expected at higher concentrations when $q\xi \gg 1$.

Experimental Procedures

All polyisoprene samples in this study were prepared by anionic polymerization and have the same stereoirregular chain microstructure (~7% 3,4; ~70% cis-1,4; ~23% trans-1,4). The stars were formed by chlorosilane-linking chemistry. The detailed procedures are described elsewhere (see ref 12). Some of their dilute-solution properties were reported elsewhere^{12,20} or determined here by low-angle laser light scattering and viscosity as described in ref 20. Those data are given in Table I. Both static and dynamic light scattering measurements were made at 25 °C with a Brookhaven photometer correlator and vertically polarized light from a He-Ne laser ($\lambda_0 = 632.8$ nm). The solvent used throughout was cyclohexane, which is a good solvent for polyisoprene ($\nu = 0.57$).²⁰

Solutions were prepared by evaporation or dilution of stock solutions. Concentrations were determined from the measured weights of polymer and solvent and then converted to w/v (g mL⁻¹) using the density of cyclohexane, $\rho = 0.7739$ g mL⁻¹ at 25 °C. All solutions were carefully filtered and equilibrated for at least 1 week prior to study. Measurements were made at 20 scattering angles, $20^\circ \leq \theta \leq 160^\circ$, corresponding to 4.90×10^{-4}

Table I
Molecular Weights and Properties of Polyisoprene Samples in Dilute Cyclohexane Solutions from Earlier Work^{10,18}

sample	architecture	$M_w \times 10^{-6}$	A_2M , mL g ⁻¹	$[\eta]$, mL g ⁻¹	R_G , Å
PI-L12	linear	0.58	360	335	395
8-X	8-arm star	0.130	90		
9-III	8-arm star	0.795	360	184	300
8-IV	8-arm star	1.76	550	325	455
18-IV	18-arm star	1.50	340	162	300
18-V	18-arm star	3.57	714	292	500
18-IX	18-arm star	6.80	1100	507	700

$\hat{A}^{-1} \leq q \leq 27.9 \times 10^{-4} \hat{A}^{-1}$. The optical constant K was calculated with the refractive index of cyclohexane, $n = 1.422$ at 25° for $\lambda_0 = 6328 \text{ Å}$, and the refractive index gradient of the system $dn/dc = 0.106 \text{ mL g}^{-1}$.²⁰

$$K = \frac{4\pi^2 n^2}{\lambda_0^4 N_A} \left(\frac{dn}{dc} \right)^2 = 9.29 \times 10^{-8} \text{ cm}^2 \text{ g}^{-1} \quad (23)$$

The excess scattering intensity at each angle was expressed in relative units, $\Delta I_r(\theta, c) = (I(\theta, c) - I(\theta, 0))/I(\theta, 0)$, and then converted to absolute units $\Delta R(\theta, c) = \Delta I_r(\theta, c) R_0$ as needed, using the Rayleigh ratio for cyclohexane, $R_0 = 5.1 \times 10^6 \text{ cm}^{-1}$.

Information about the dynamic structure factor was obtained by a second-order cumulant fit of the intensity correlation function, providing the first and second cumulants Γ and Γ^2 . Data were judged to be acceptable only when the calculated base line (from the monitor channels) and the measured base line (from the delayed channels) agreed within 1 part in a thousand. The coefficient ζ was always smaller than 0.1 except near c^* where the spectrum was broader and gave values as large as 0.3. Further investigation would be needed to determine the exact profile of the dynamical structure factor around c^* .

The first cumulant was obtained using $\pm 20\%$ variations in the correlator time window around the value $\Delta t = 3/\Gamma$. We estimate an uncertainty of 4% in $\Gamma(q, c)$. The variation of $\Gamma(q, c)/q^2$ with q was studied at each concentration. When necessary, the results were extrapolated to $q = 0$ according to eq 15 to obtain $D(c)$. Values of $D(c)$ in the dilute range were used to extract D_0 (eq 13).

Results and Discussion

Behavior in the three regimes of concentration—dilute ($c \ll c^*$), semidilute ($c \gg c^*$), and near overlap ($c \sim c^*$)—is discussed separately. The definition of c^* based on the second virial coefficient (eq 10) was used in most cases.

1. Dilute Solutions. Examples showing $[\Delta I_r(\theta, c)]^{-1}$ as a function of $\sin^2(\theta/2) \propto q^2$ are given for solutions of two stars in the dilute regime in Figure 1. The dependence is linear when $qR_G < 1$, as expected, with departures from linearity at larger values of qR_G , also as expected and as observed in dilute solutions of linear polymers.

Examples of $D(q, c)/D(0, c)$ as a function of $q^2 R_G^2$ in dilute solutions are given in Figure 2. Here the behavior for linear polymers and stars is quite different. In linear polymers the values of $D(q, c)$ begin to increase beyond $qR_G \sim 1$, showing the contribution of internal modes. In star polymers $D(q, c)$ remains essentially independent of q even up to $qR_G \sim 2$. Indeed, scattering in this q range has been suggested to reflect not the interior structure of the star but rather its well-defined surface.³ The dominant motion of this surface is expected to depend primarily on the overall translational diffusion of the star. This is consistent with our observations and those obtained at somewhat higher reduced concentrations by neutron scattering.¹⁰

We note finally a distinct difference in $D(c)$ vs c behavior for linear and star polymers in the dilute range. Thus, $D(c)$ starts with a definite slope for linear polymers but remains essentially constant for stars ($k_D \sim 0$, within the error bounds here) at the lowest reduced concentrations ($0.04 < A_2Mc < 0.4$). Since $k_D = 2A_2M - k_s$, this result

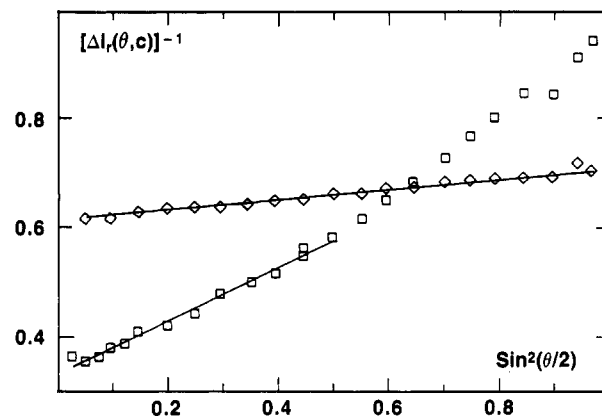


Figure 1. Examples showing the angular dependence of relative scattering intensity for star polymers in the dilute regime. Values of $[\Delta I_r(\theta, c)]^{-1}$ vs $\sin^2(\theta/2)$ are shown for sample 8-III at $c = 4.82 \times 10^{-4} \text{ g mL}^{-1}$ (\diamond) (the values of $(\Delta I_r)^{-1}$ in this case were multiplied by a factor of 2 for clarity), and for sample 18-IX at $c = 4.70 \times 10^{-5} \text{ g mL}^{-1}$ (\square). The lines drawn correspond to $R_G = 250 \pm 10 \text{ Å}$ and $\Delta I_r(0, c) = 3.78 \pm 0.03$ for 8-III and to $R_G = 740 \pm 40 \text{ Å}$ and $\Delta I_r(0, c) = 3.00 \pm 0.08$ for 18-IX (fitted in the range $0.47 \leq qR_G \leq 1.48$ for the latter).

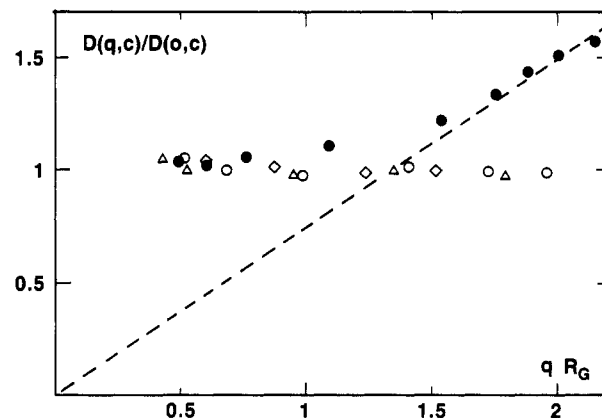


Figure 2. Examples comparing the angular dependence of mutual diffusion coefficient for linear and star polymers in the dilute range. Values of $D(q, c)/D(0, c)$ vs qR_G are shown for a linear polystyrene sample (Toya Soda, $M = 2.89 \times 10^6$) in toluene (\bullet) and a polyisoprene star sample, 18-IX, at three concentrations in the range $0.05 < MA_2c < 0.2$ (\diamond , Δ , \circ). The dashed line is used to emphasize that $D(q, c)/D(0, c) \sim qR_G$ near $qR_G \sim 2$ for a linear polymer in dilute solution, as expected from eq 18, while remaining independent of qR_G in the same range for a star.

implies a larger frictional interaction between stars at constant A_2Mc in the dilute range. A similar enhancement is found when k_s is calculated from earlier data on linear²⁰ and star¹² polyisoprenes, a behavior that is perhaps related to the increase in Huggins coefficient k_H with increasing branch number noted previously.¹² A similar decreasing trend in k_D with branch number can be seen in data for polystyrene stars.⁶

2. Semidilute Solutions. The concentration derivative of osmotic pressure $\partial\pi/\partial c$ was obtained by extrapolation of $Kc/\Delta R(q, c)$ to $q = 0$ (eqs 5 and 6). The results are shown as a function of polymer concentration in Figure 3. For the samples used here, $\partial\pi/\partial c$ vs c becomes independent of the chain architecture beyond $c \sim 0.01 \text{ g mL}^{-1}$, and all data merge to a single power law

$$\frac{1}{RT} \frac{\partial\pi}{\partial c} = (1.0 \pm 0.1) \times 10^{-2} c^{1.32 \pm 0.02} \quad (24)$$

where c is measured in units of grams per milliliter. According to scaling ideas, the exponent is $(3\nu - 1)^{-1}$, leading to $\nu = 0.586 \pm 0.006$, which agrees very well with the self-

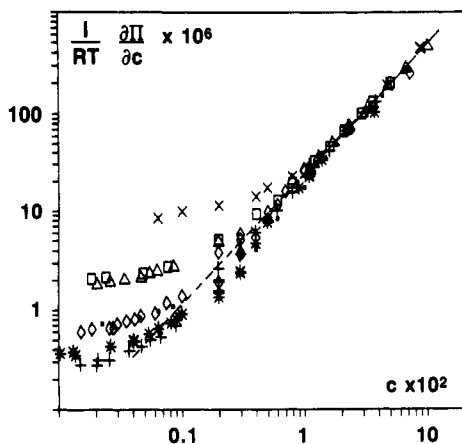


Figure 3. Variation of the osmotic pressure derivative with concentration for linear and star polyisoprenes. Results are shown for linear polyisoprene (PI-15 (Δ)), 8-arm stars (8-X (\times), 8-III (\square), 8-IV (\diamond)), and 18-arm stars (18-IV (\blacksquare), 18-V ($*$), 18-IX ($+$)). As noted in the text, $\partial\pi/\partial c$ becomes independent of chain architecture for $c > 10^{-2}$ g mL $^{-1}$. The dashed line corresponds with eq 24 in the text.

avoiding chain prediction of $\nu = 0.588$. It also agrees well with the exponent found for poly(α -methylstyrene) in toluene.¹⁴

Two aspects of the results shown in Figure 3 are noteworthy. First, the distinction between the linear and star architectures vanishes in the semidilute range. The values of $\partial\pi/\partial c$ depend only upon c , and scattering intensity is insensitive to q in the concentration range where $q\xi \ll 1$. These observations are consistent with other data for polymers in good solvents and nicely support the Daoud-Cotton model for stars. From eqs 4 and 24 we obtain an expression for the correlation length:

$$\xi = 7.4c^{-0.77 \pm 0.01} \text{ (\AA)} \quad (25)$$

Second, there is a difference among chain architectures when the data are plotted in reduced form, $(\partial\pi/\partial c)/(\partial\pi/\partial c)_0 = (\partial\pi/\partial c)M/RT$ vs MA_2c , as in Figure 4. On the other hand, the results for all polymers having the same number of arms lie along the same curve. The three lines in Figure 4 correspond to linear, 8-arm, and 18-arm polymers

$$\frac{M}{RT} \frac{\partial\pi}{\partial c} = 2.5(MA_2c)^{1.30} \text{ (linear)} \quad (26a)$$

$$\frac{M}{RT} \frac{\partial\pi}{\partial c} = 3.1(MA_2c)^{1.30} \text{ (8-arm)} \quad (26b)$$

$$\frac{M}{RT} \frac{\partial\pi}{\partial c} = 4.6(MA_2c)^{1.32} \text{ (18-arm)} \quad (26c)$$

with uncertainties of 10% in the prefactors and 5% in the exponents.

Equation 26a includes also the data reported in ref 14 for poly(α -methylstyrene) in toluene:²¹ the curve for linear polymers appears to be the same in both systems. The exponents for different architectures agree and are consistent with eq 24. The prefactors differ and increase with f as expected, but the variation with f is weaker than predicted. Thus, the prefactor for 18-arm stars is only 1.5 times larger than that for 8-arm stars, whereas we expect $(18/8)^{3/2} = 3.4$. A similar difference is found when the data are compared with prefactors calculated by renormalization group methods.²² In that case the predicted prefactor ratio for 6-arm stars relative to linear chains is

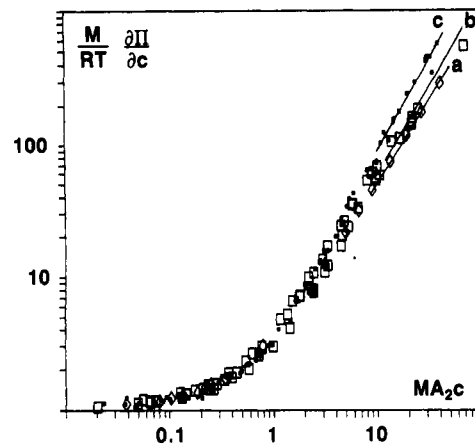


Figure 4. Reduced osmotic pressure derivative as a function of reduced concentration MA_2c . The symbols correspond to linear (\diamond), 8-arm stars (\square), and 18-arm stars (\blacksquare). Lines a-c correspond to eqs 26a-c in the text, respectively.

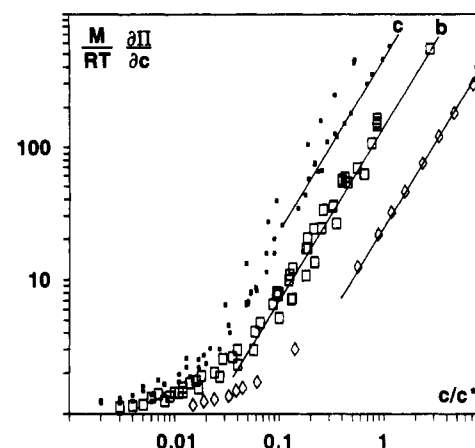


Figure 5. Reduced osmotic pressure derivative as a function of reduced concentration $N_a R_G^3 c / M$. Symbols have the same meaning as those in Figure 4. The prefactors corresponding to lines a (linear), b (8-arm), and c (18-arm) are 25, 150, and 470, respectively.

2.05, which is already larger than the experimental ratio of $3.1/2.5 = 1.24$ for 8-arm stars.

Some of this discrepancy may be due to the choice of $(MA_2)^{-1}$ as c^* in the reduction procedure (eq 10). The more conventional definition is $M/N_a R_G^3$ (eq 9), but we have avoided that because the errors in R_G^3 are so much larger, and for most purposes the choice is arbitrary anyway. The data are replotted in Figure 5 with $c^* = M/N_a R_G^3$ as the reduction variable. The results are indeed more scattered than those in Figure 4, and the attractive feature of superposition in the dilute range is lost. The prefactors (as best they can be estimated in this case) seem now, however, to be more consistent with the predicted $f^{3/2}$ dependence. Nonetheless, the choice in c^* definition is still an arbitrary one, and the differences (apart from the greater experimental uncertainty in R_G^3 than in MA_2) are traceable directly to the arm number dependence of $(M/R_G^3)/(MA_2)^{-1} = M^2 A_2 / R_G^3$, which changes with f and only attains a constant value for $f > 30$.¹² Finally, to emphasize the point, we can write our result in the general form

$$\frac{M}{RT} \frac{\partial\pi}{\partial c} = BF(f) (c/c^*)^{1/(3\nu-1)} \quad (27)$$

where B is the prefactor for linear chains. The function $F(f)$ cancels the f dependence of c^* , however defined, in order to render $\partial\pi/\partial c$ independent of both arm number

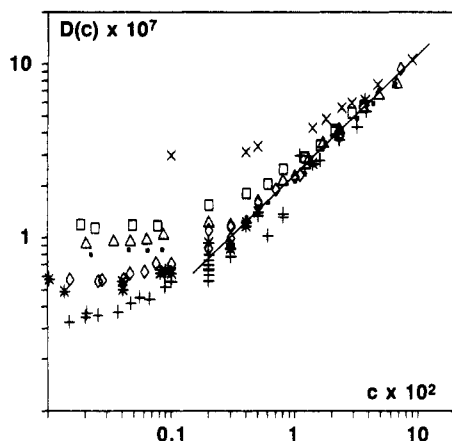


Figure 6. Variation of the mutual diffusion coefficient with concentration for linear and star polyisoprenes. Symbols have the same meaning as those in Figure 3. The line corresponds with eq 28 in the text.

and molecular weight in the semidilute regime. Removing ambiguities related to the definition of c^* , and providing clear tests of the predicted $f^{3/2}$ prefactor dependence, would appear to require data on stars with many more arms.

Similar issues arise in the analysis of dynamical behavior. The mutual diffusion coefficient is shown as a function of concentration in Figure 6. Results for the various chain architectures merge to a common curve at high concentrations, although with somewhat more scatter than the $\partial\pi/\partial c$ results (Figure 3). The values of $D(c)$ can be described by a power law for $c > 0.01$ g mL $^{-1}$:

$$D(c) = (5.5 \pm 0.8) \times 10^{-6} c^{0.69 \pm 0.03} \quad (\text{cm}^2 \text{ s}^{-1}) \quad (28)$$

(The data for sample 8-X are only just approaching this asymptote at $c = 0.01$ g mL $^{-1}$ and were omitted in the determination of eq 28). The effects of chain architecture vanish in the semidilute range, and we obtain simply the mutual diffusion coefficient for a correlation volume whose mobility depends on concentration alone. The exponent is somewhat smaller than the expected value of 0.77 from eq 19. The result is similar to the law found for semidilute solutions of linear polystyrene in benzene ($D(c) \propto c^{0.67}$).²³

The same data are plotted in reduced form, $D(c)/D_0$ vs MA_2c in Figure 7. The results for most samples are consistent with a single asymptote. The line in Figure 7 corresponds to the best fit using all the experimental results

$$D(c)/D_0 = 1.0(MA_2c)^{0.68}$$

with an uncertainty of 13% in the prefactor and 3% in the exponent. Thus, in apparent contrast with the osmotic pressure derivatives, the diffusion coefficients for linear and star polymers seem to follow the same curve when plotted in reduced form. However, from our earlier discussion we expect a much smaller variation with f in the prefactor for reduced diffusion coefficient ($f^{1/2}$) than for the reduced osmotic pressure derivative ($f^{3/2}$). We have also shown that the latter varies less strongly than predicted, so it is not surprising that an f variation in $D(c)/D_0$ cannot be seen experimentally.

3. Solutions near the Overlap Concentration. If a liquidlike ordering of stars occurs near c^* , as suggested in ref 4, the scattering intensity $\Delta I_r(q, c)$ for $c \sim (MA_2)^{-1}$ should pass through a maximum in the vicinity of $q = R_G^{-1}$.²⁴ Results for the largest 18-arm star, sample 18-IX, are shown in Figure 8 at reduced concentrations of $MA_2c = 0.47, 0.89, 1.10$, and 5.0 . The intensity decreases monotonically with q for the lowest concentration and

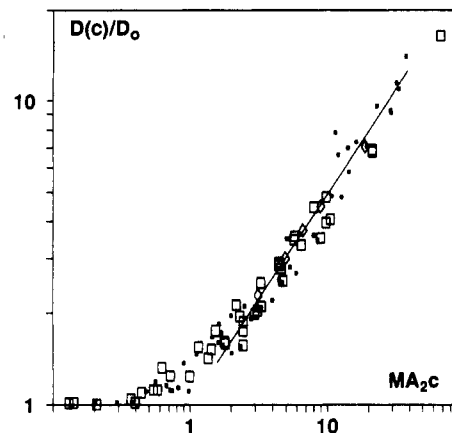


Figure 7. Reduced mutual diffusion coefficient as a function of the reduced concentration MA_2c . Symbols have the same meaning as those in Figure 4. The line corresponds with eq 29 in the text.

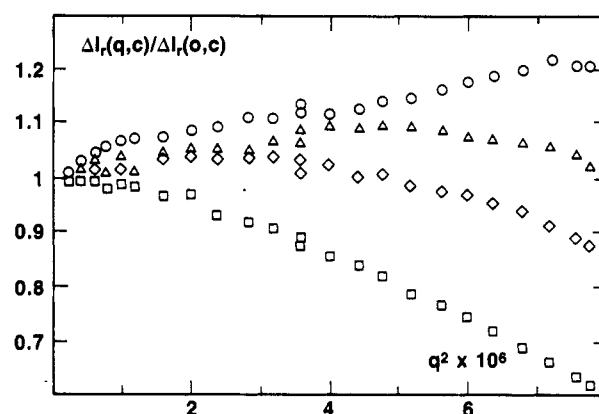


Figure 8. q dependence of the reduced relative scattering intensity for star sample 18-IX at four concentrations bracketing the overlap region. The concentrations correspond to MA_2c values of 0.47 (\square), 0.89 (\diamond), 1.1 (\triangle), and 5.0 (\circ); q^2 is equal to 1.8×10^{-6} (\AA^{-2}) at $qR_G = 1$.

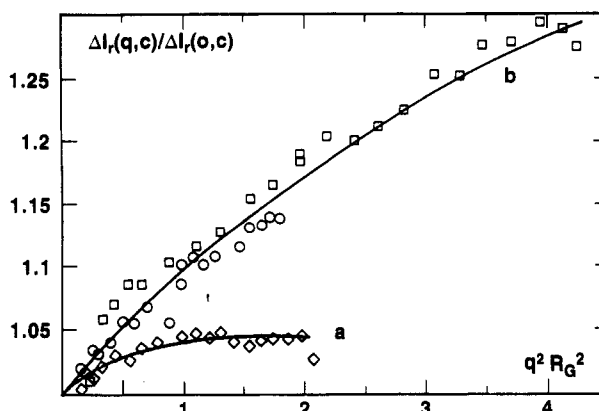


Figure 9. Reduced relative scattering intensity as a function of $q^2 R_G^2$ for star polyisoprenes at $MA_2c \approx 2.0$. The symbols correspond to an 8-arm star (8-IV (\diamond)) and two 18-arm stars (18-V (\circ), 18-IX (\square)). Curves a (8-arm) and b (18-arm) are meant merely as guides for the eye.

increases monotonically for the highest concentration, but there indeed appears to be a shallow maximum for the two intermediate concentrations. The result is in good agreement with ref 7, in which maxima were found near c^* by neutron scattering (compatible with liquidlike ordering, $q_{\text{max}} \propto c^{-1/3}$) for two 12-arm polystyrene stars.

In Figure 9 the normalized intensity $\Delta I_r(q, c)/\Delta I_r(0, c)$ is plotted as a function of $q^2 R_G^2$ for three stars, each at a

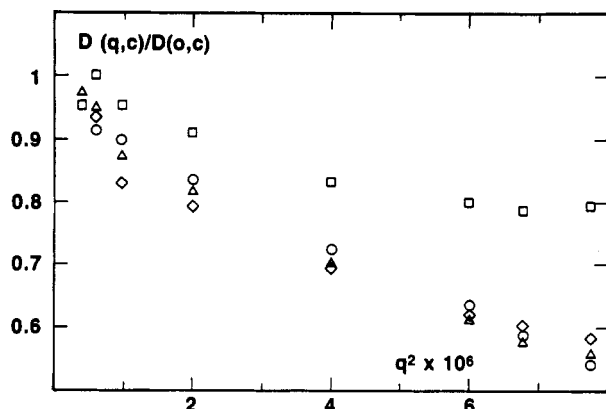


Figure 10. q dependence of the reduced mutual diffusion coefficient for star sample 18-IX at four concentrations bracketing the overlap region. Symbols have the same meaning as those in Figure 8.

concentration such that $MA_{2c} = 2 (\pm 10\%)$. The two 18-arm stars follow the same curve. Thus qR_G is the correct reduced variable for the static structure factor at this concentration, indicating that the maximum will indeed appear near $q = R_G^{-1}$. The curve for the 18-arm stars is higher than the curve for the 8-arm star, suggesting that the scattering maximum increases and the ordering becomes more pronounced as the arm number increases. It would be desirable to work with stars with larger radii and higher functionality in order to establish more precisely how q_{\max} and the sharpness of the maximum vary with c/c^* , R_G , and f .

There is other evidence that suggests the existence of a repulsion between stars near c^* . In this range the values of $\partial\pi/\partial c$ for 18-arm stars lie below the semidilute law (eq 25). Thus, a linear polyisoprene with $M = 4.4 \times 10^6$ (the molecular weight of sample 18-IX) would follow that law down to $c \approx 6 \times 10^{-4}$ g mL $^{-1}$ and, from Figure 3, would have larger values of $\partial\pi/\partial c$ than the star. This agrees qualitatively with the prediction⁴ that $\partial\pi/\partial c \approx RT/Mf^{1/2}$ near c^* .

The dynamical behavior also suggests an extra interaction between stars near c^* . The values of $D(q,c)$ are strongly q dependent and decrease with increasing q . The results, expressed as $D(q,c)/D(0,c)$ vs q^2 , are shown in Figure 10 for sample 18-IX at $MA_{2c} = 0.47, 0.89, 1.10$, and 5.0 (the same solutions as in Figure 8). The decrease with q was observed near c^* in all star samples except the smallest (8-X). For the linear sample, PI-12, $D(q,c)$ is independent of q at $MA_{2c} = 0.8$ ($D(q,c)/D(0,c) = 1.22 \pm 0.03$ in the range $5.4 \times 10^{-7} < q^2 (\text{\AA}^{-2}) < 4 \times 10^{-6}$). For the solution of lowest concentration in Figure 10, $D(q,c)$ first decreases and then appears to become essentially constant ($q^2 (\text{\AA}^{-2}) > 6.8 \times 10^{-6}$, $qR_G > 2$). The static structure factor is still a monotonically decreasing function of q at this concentration (see Figure 8), so the dynamical behavior is more sensitive to c^* ordering than the static behavior. Dynamic neutron scattering experiments^{9,10} have been reported for stars in the overlap range ($1.6 < MA_{2c} < 3.4$ in ref 8). Those data were analyzed as though the solutions were dilute, but the behavior might, in fact, be more closely related to c^* ordering than to single-chain properties.

From the measurements of $S(q,c)$ and $D(q,c)$ one can obtain $\mu(q,c)$, the mobility per unit mass of polymer (eq 20). For $qR_G > 1$ and in the concentration range $0.5 < MA_{2c} < 5$, $\mu(q,c)$ decreases monotonically with increasing q , as in the case of a linear polymer. No new information is obtained.

Summary and Conclusions

We have used light scattering to investigate the static and dynamic properties of multiarm star polyisoprenes in a good solvent, cyclohexane. Measurements were made on one linear polymer, three 8-arm stars, and three 18-arm stars in three concentration regimes—dilute, semidilute, and near the crossover. Several features distinguishing linear and star polymer behavior were observed.

In dilute solutions the diffusion coefficient for stars was independent of the scattering vector even out to $q \sim 2/R_G$. Thus, unlike linear chains, stars do not exhibit internal motions strongly in this q range. This is the behavior expected of rigid scatterers. Thus the concentration dependence of mutual diffusion departs from that of linear polymers and approaches that of hard spheres.

This behavior of stars as rigid impenetrable particles is lost in the semidilute regime. The scattering behavior reverts to that of a linear polymer at the same concentration. Both the scattering intensity and its dynamics become independent of molecular architecture and are functions of concentration alone. The power laws obtained for the concentration dependence of the osmotic pressure derivative and cooperative diffusion coefficient agree well with the data on other polymers in good solvents. On the other hand, the various architectures do not obey the expected semidilute scaling laws: both $\partial\pi/\partial c/(\partial\pi/\partial c)_0$ and $D(c)/D_0$ depend more weakly than predicted on the number of arms for a given value of c/c^* .

Evidence was found supporting the idea of liquidlike ordering for stars in the region near c^* . The q dependence of scattering intensity shows a weak maximum near $q = R_G^{-1}$ but is monotonic at concentrations well below and well above c^* . The q dependence of $D(q,c)$ near c^* is qualitatively different for linear chains and stars and is consistent with c^* ordering as well.

Acknowledgment. We thank P. Pincus for stimulating discussions and Eli Habeeb and Andrea Kiss for assistance with the experimental work. The help provided by one of the reviewers is also very much appreciated. Also, M.A. expresses gratitude to P. Berge, CEN-Saclay, for permitting her an extended leave and to R. R. Chance for the opportunity to work at the Exxon Corporate Laboratories.

References and Notes

- (1) Permanent addresses: (a) SRM, SEN-Saclay, 91191 Gif-sur-Yvette Cedex, France. (b) Department of Chemical Engineering, Princeton University, Princeton, NJ 08544. (c) Department of Physics, University of Chicago, Chicago, IL 60601.
- (2) Daoud, M.; Cotton, J. P. *J. Phys. (Paris)* **1982**, *43*, 531.
- (3) Grest, G. C.; Kremer, K.; Witten, T. A. *Macromolecules* **1987**, *20*, 1376.
- (4) Grest, G. C.; Kremer, K.; Milner, S. T.; Witten, T. A. *Macromolecules* **1989**, *22*, 1904.
- (5) Witten, T. A.; Pincus, P. A.; Cates, M. E. *Europhys. Lett.* **1986**, *2*, 137. See also: Witten, T. A.; Pincus, P. A. *Macromolecules* **1986**, *19*, 2509.
- (6) Huber, H.; Burchard, W.; Fetters, L. J. *Macromolecules* **1984**, *17*, 541.
- (7) Huber, K.; Bantle, S.; Burchard, W.; Fetters, L. J. *Macromolecules* **1986**, *19*, 1404.
- (8) Richter, D.; Stuhn, B.; Ewen, B.; Nerger, D. *Phys. Rev. Lett.* **1987**, *58*, 2462.
- (9) Burchard, W. *Makromol. Chem., Makromol. Symp.* **1988**, *18*, 1.
- (10) Richter, D.; Farago, B.; Huang, J. S.; Fetters, L. J.; Ewen, B. *Macromolecules* **1989**, *22*, 468.

- (11) Roovers, J.; Toporowski, P.; Martin J. *Macromolecules* **1989**, *22*, 1897.
- (12) Bauer, B. J.; Fetters, L. J.; Graessley, W. W.; Hadjichristidis, N.; Quack, G. *Macromolecules* **1989**, *22*, 2337.
- (13) Le Guillou, J. C.; Zinn-Justin, J. *Phys. Rev.* **1980**, *21*, 3976. See also: Cotton, J. P. *J. Phys. Lett.* **1980**, *41*, L231.
- (14) Noda, T.; Kato, N.; Kitano, T.; Nagasawa, M. *Macromolecules* **1981**, *14*, 668.
- (15) Wiltzius, P.; Haller, H. R.; Cannell, D. S.; Schaefer, D. W. *Phys. Rev. Lett.* **1983**, *51*, 1183.
- (16) Chu, B. *Laser Light Scattering*; Academic Press: New York, 1974.
- (17) Yamakawa, H. *Modern Theory of Polymer Solutions*; Harper & Row: New York, 1971.
- (18) de Gennes, P.-G. *Scaling Concepts in Polymer Physics*; Cornell University Press: Ithaca, NY, 1979.
- (19) Adam, M.; Delsanti, M. *J. Phys. Lett.* **1977**, *28L*, 271.
- (20) Davidson, N. S.; Fetters, L. J.; Funk, W. G.; Hadjichristidis, N.; Graessley, W. W. *Macromolecules* **1987**, *20*, 2614.
- (21) Equation 26a was obtained from the data in ref 14 (their Tables I and III with MA_2 deduced from their eqs 14 and 24, leading to $MA_2 = 6.7 \times 10^{-3} M^{0.756}$).
- (22) Cherayil, B. J.; Bawendi, M. G.; Miyake, A.; Freed, K. F. *Macromolecules* **1986**, *19*, 2770.
- (23) Adam, M.; Delsanti, M. *Macromolecules* **1977**, *10*, 1229.
- (24) We note that similar intensity maxima were reported for a linear poly(α -methylstyrene) sample near c^* ,²⁵ but this result clearly contradicts many other data for linear polymers in good solvents,^{15,26,27} where no maximum was observed.
- (25) Kim, S. H.; Ramsey, D. J.; Patterson, G. D.; Selser, J. C. *Polym. Prepr. (Am. Chem. Soc., Div. Polym. Chem.)* **1987**, *28*, (1), 363.
- (26) Dautzenberg, H. *J. Polym. Sci., Polym. Symp.* **1977**, *61*, 83.
- (27) Hager, B. L.; Berry, G. C.; Tsai, H.-H. *J. Polym. Sci., Part B: Polym. Phys.* **1987**, *25*, 387.

Registry No. Cyclohexane, 110-82-7; polyisoprene, 9003-31-0.